

## (B1) SCALING

**(b1.1) Hessian calculation****Choice of optimal point**

As mentioned in A3, the gradient method struggled a lot finding an optimal point, as all gradient evaluated at the points found were non-zero. This has to do with the termination condition of the gradient function used: *fmincon*. This function, based on the quasi-newton method, stops when the step it takes get within a certain threshold, as opposed to checking that the gradient at a certain point is zero - which would be much more computationally expensive.

To get a better outcome from the gradient optimization, the initial point from which the search method starts was taken from the pareto front found in (b2). This point might not be optimal for the gradient search though, since the cost function is a single objective comprising the combination of not only LoD and the weight, but also the costs due to the penalty function as discussed in A3.

$$Penalty = -LoD + fuelCost + liftCost + deltaCost + weightCost$$

The table below shows the initial guess: the Pareto Front point maximizing weight, and then the gradient optimized point for the penalty function:

Design variable	b	c	l	a1	a2	a3	a4	a5	a6
<b>Start point (PF)</b>	0.96	1.16	0.10	-1.55	-2.20	-3.37	-2.60	-1.16	-0.89
<b>Optimized point</b>	0.95	1.03	0.096	-1.54	-1.01	-1.01	-1.01	-1.16	-0.89

The following table shows the performance comparison:

Performance	LoD	Weight (N)	Lift (N)	Volume (m3)	Tip deflection(ft)	Penalty
<b>Start point</b>	51.6	337	350	0.0271	2.8078	103.4668
<b>Optimized point</b>	50.4	347	347	0.0213	3.0600	-42.3007

As can be seen, one of the Pareto optimal point is far from optimal in terms of the penalty function. This is because when the Pareto points were evaluated, instead of requiring the weight and the lift to match exactly, a slack of 5% was introduced, to discard less points - more details on this in (b2). This discrepancy in lift is however a very heavy weight constraint in the penalty function, drawing the cost up by a lot.

## Setup

To calculate the Hessian, finite differences were combined with Romberg Extrapolations, as developed by D'Errico in his MATLAB toolbox. This toolbox provides a function implementing an adaptive method to compute accurate numerical Hessians. The specific settings used were:

- Method order: 4
- Finite difference type: central
- Romberg terms: 2
- Max step: 0.2 - this was enforced to bound the states used for calculating the Hessian.

It is important to note that this method is very computationally expensive, and hence would not be very useful for gradient methods.

## Results

The table below shows the diagonal Hessian entries:

Design variable	$b$	$c$	$l$	$\alpha_1$	$\alpha_2$	$\alpha_3$	$\alpha_4$	$\alpha_5$	$\alpha_6$
Hessian	-10.59	$2.39 \cdot 10^5$	-2.75	0	0	0	0	0	0

### (b1.2) Scaling factors

The last six variables have zero valued Hessians, meaning that in the neighborhood around points with infinitesimally small changes in  $\alpha$ , the penalty function is a hyperplane and has no “curvature”. Hence the scaling factor could only be a matter of consideration for the three first design variables. The only design variable with an order of magnitude larger than 100, is the chord,  $c$ , with a Hessian in the order of magnitude of  $10^5$ . Hence a scaling factor of  $10^2$  would be desired,  $c' = 100 \cdot c$ .

### (b1.3) Scaling results

The gradient optimization algorithm was run with the change of variable discussed in b1.2, where yellow means the variable was calculated, and the orange that the state was scaled back at the end.

Design variable	$b$	$c$	$c'$	$l$	$a_1$	$a_2$	$a_3$	$a_4$	$a_5$	$a_6$
Start point	0.95	1.03	103	0.096	-1.54	-1.01	-1.01	-1.01	-1.16	-0.89
Optimized point	0.95	1.03	103	0.096	-1.54	-1.01	-1.01	-1.01	-1.16	-0.89

Nevertheless, as can be seen, the scaling did not seem to change the outcome with the search function being used.

## (b2) Multiobjective Optimization

We optimized our wing for two objective functions, which were:

- Wing weight
- Lift-over-drag.

To do so, we had to be clever about the way we searched the design space. Having 9 continuous variables to explore, and costly evaluation functions made us think hard about how to efficiently search the design space. As a refresher, our design variables were:

- Normalized span
- Normalized root chord
- Taper ratio
- 6 angles of attack spaced across the wing

The constraints imposed were:

- Lift
- Tip deflection
- Fuel volume

From A3, we were able to determine an angle of attack distribution through a particle swarm optimization that resulted in a lift distribution with high L/D. However, the planform design was yet to be determined since the penalty functions implemented in the A3 methods were not effective in helping find designs that satisfied all of the constraints.

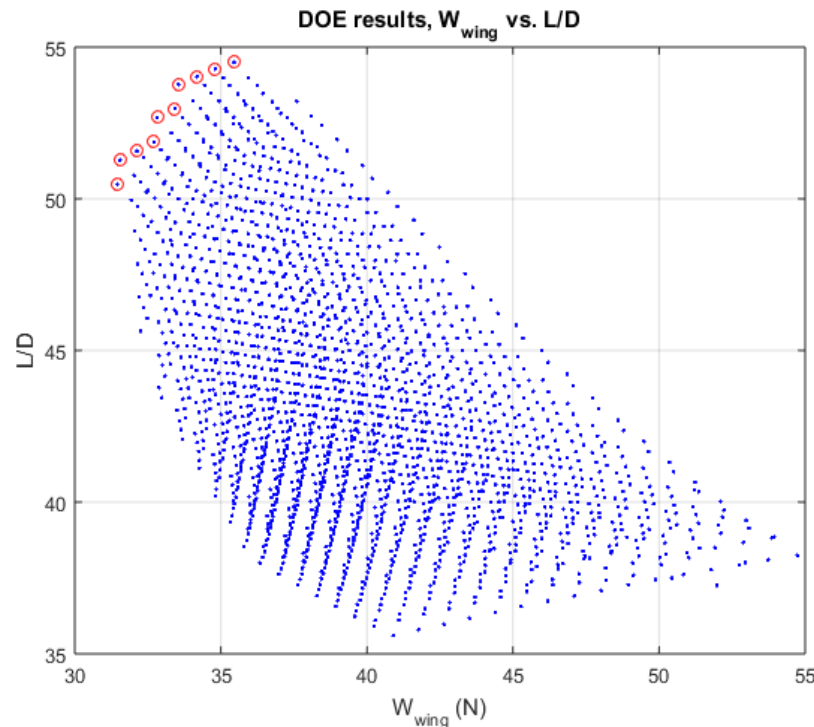
Making the assumption that the planform design and angle of attack distribution could be designed in parallel instead of synergistically, we performed a design of experiments on the span, root chord and the taper ratio, using the angles found from our heuristic optimization method from Assignment 3. The bounds for the three design variables for the DOE are below.

- Normalized span: [0.85 : 1.15]
- Normalized root chord: [0.8 : 1.2]
- Taper ratio: [0.1 : 1]

The space between the bounds for each variable were linearly sampled 20 times, yielding  $20 \times 20 \times 20 = 8000$  different planform designs for the aircraft. As expected, not all of these designs fulfilled the three constraints defined by the overall aircraft configuration. We wrote a function to prune the DOE for the wings that violated the tip deflection and fuel volume constraints, as well as attaining at least 95% of the lift constraint. The reason a relaxation was added to the third constraint is because the lift of the wing can also be modified through changes in the angle of attack distribution.

At the end, 2167 wings out of 8000 were found to fulfill the two constraints + one relaxed constraint. Afterwards, a logarithmic-weighted sum function was run on the feasible solutions to find the Pareto front. Surprisingly, there were only 4 Pareto-optimal wings found, and it was observed that some concave sections of the frontier were not shown to be Pareto-optimal.

However, it was possible that they were also part of the non-dominated set of solutions. Therefore, another function (courtesy of Eduard Polityko) was run to find the non-dominated set of results, giving the actual Pareto front of the DOE, which consists of 10 distinct wing planforms plotted in red below.



**(b2.1)** The shape of the Pareto front is multimodal, which means that it has both convex and concave sections.

**(b2.3)** The design of the wing planform was not subject to scaling problems, since it was explored through a full factorial DOE. The design space was small enough for the 3 parameters that the 8000 item DOE was performed within 10 hours.

**(b2.4)** We could select a final design from the Pareto front by integrating another kind of analysis on top of the wing performance based optimization. When arguing for a specific wing design, we must take into account the effects of wing performance on overall aircraft performance, which are obviously significant.

In the initial sizing of the aircraft, the objective was to minimize MTOW given a large number of constraints and variables. This sizing implemented a convex optimization algorithm, which made a number of conservative wing performance assumptions to ensure that the design was attainable. Therefore, it is predicted that the optimized wing design would result in improvements in the primary goal of minimizing MTOW.

L/D and weight of the wing are objectives of the wing optimization, which is a subproblem of the aircraft system optimization. They can be related directly to the primary optimization objective

(MTOW) through a number of sensitivities returned by the system optimization. Through some clever manipulations of these sensitivities, we can evaluate the sensitivity of the MTOW of the aircraft to the wing performance parameters.

The two sensitivities of interest were:

- Sensitivity to gravity: 1.09
- Sensitivity to cruise velocity: 0.318

At first glance, it may not seem useful to find the sensitivity of the design to gravitational acceleration, since it is fixed and beyond the control of the designers. But in this case, it turns out to be very valuable. It allows us to find the sensitivity of the design to changes in component weights. Through a simple expression we can relate the relative change in wing weight to the relative change in the MTOW of the aircraft.

$$S_{W_{wing}} = S_g \cdot \frac{W_{wing_{ref}}}{MTOW_{ref}} = 0.0939$$

Furthermore, we can relate the L/D to the cruise velocity. Drag is proportional to the square of the speed, but lift is constant during steady level flight. As a result, the sensitivity of MTOW to the L/D is:

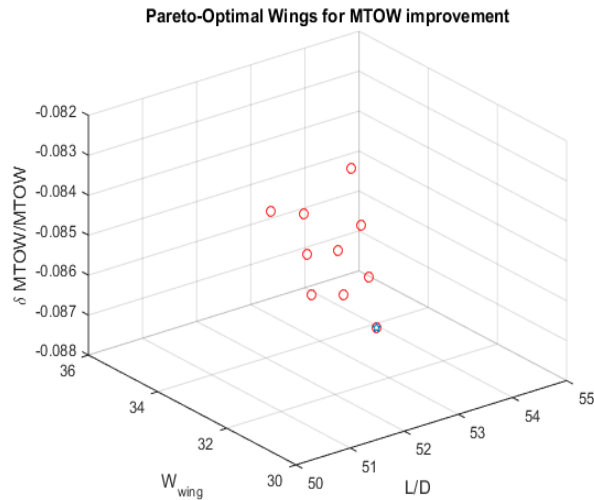
$$S_{L/D} = -0.5S_V = -0.159$$

Using these sensitivities on the Pareto-optimal wing designs, we can estimate the relative decrease (or increase) in the objective function (MTOW) that results from each design. Then, we can identify the singular design that results in the greater improvement in MTOW, and conclude that this is the best wing to satisfy the primary objective, and therefore should be the singular design offered by the wing optimization program.

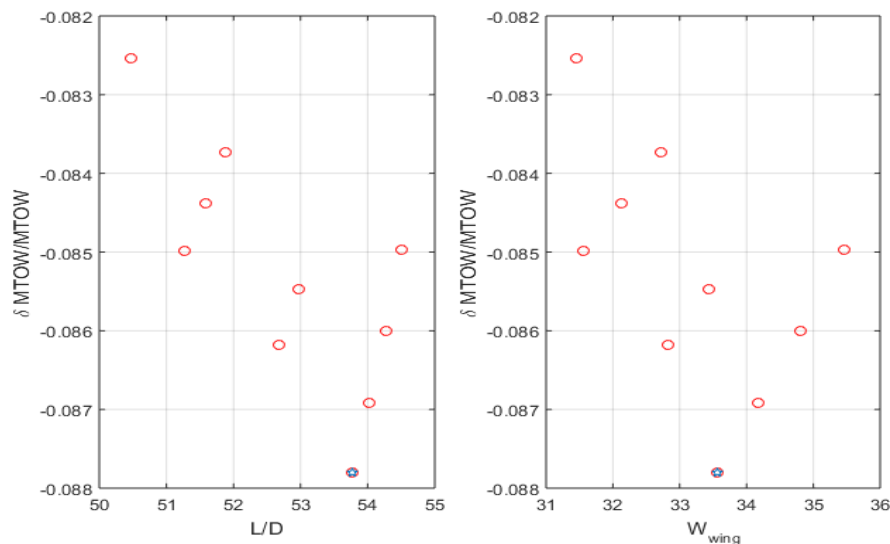
The performance of the ten Pareto-optimal designs is shown below. The chosen design is highlighted in green, and confers the greatest fractional reduction in MTOW.

<b>L/D</b>	<b>Wing weight (N)</b>	<b>dMTOW/MTOW</b>	<b>Wing Index</b>
<b>53.8</b>	33.6	-0.0878	1600
<b>54.0</b>	34.2	-0.0869	913
<b>52.7</b>	32.8	-0.0862	1150
<b>54.3</b>	34.8	-0.0860	663
<b>53.0</b>	33.4	-0.0855	672
<b>51.3</b>	31.6	-0.0850	794
<b>54.5</b>	35.5	-0.0850	1386
<b>51.6</b>	32.1	-0.0844	182
<b>51.9</b>	32.7	-0.0837	951

Here are some plots of the data to help visualize the L/D and weight tradeoffs for the wings.



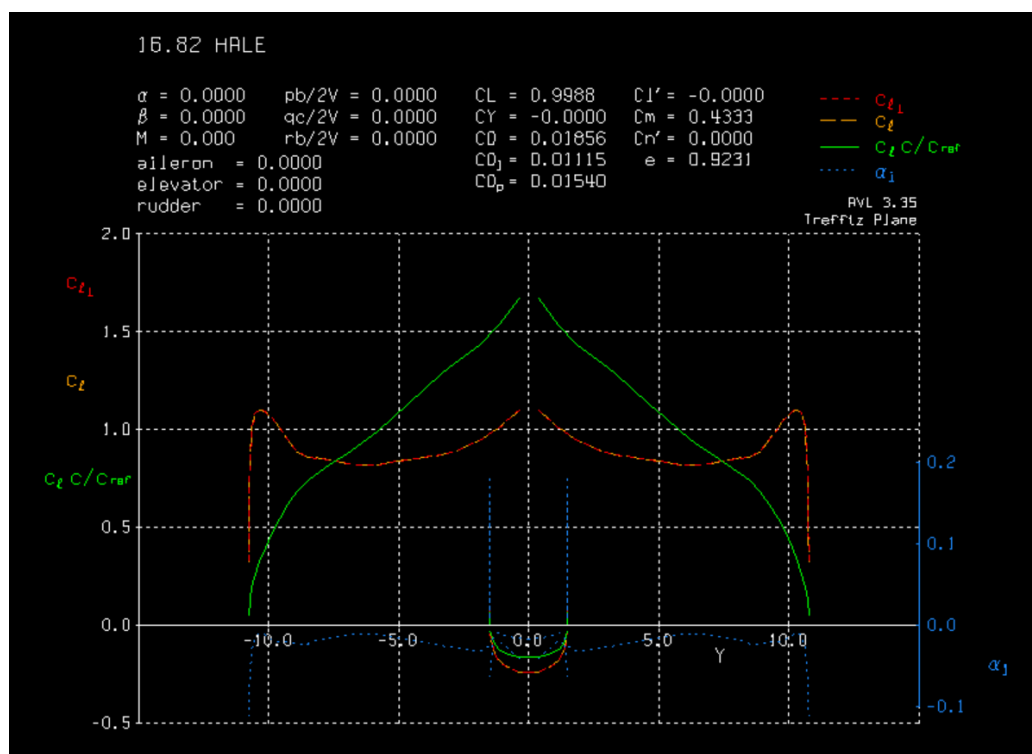
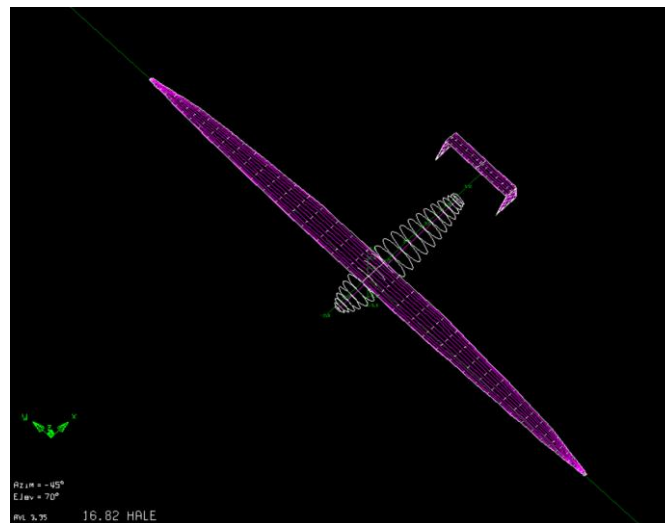
Above is a 3D plot showing the two subproblem objectives, L/D and  $W_{\text{wing}}$ , against the relative decrease in MTOW. Unfortunately, it is difficult to see the hyperplane that is formed by the points. To help visualize, the decrease in MTOW has been plotted below against L/D and  $W_{\text{wing}}$  below.



This is a really interesting result that shows the power of multidisciplinary design optimization.

It is obvious to an aircraft designer that lower wing loading results in a greater lift-over-drag. However, as the wing loading decreases, the wing must necessarily get heavier, and it is not obvious where the benefits of better L/D are outweighed by the costs of greater wing weight due to structural constraints. This graph shows exactly where the cutoff is for the tradeoff for minimizing MTOW.

As a reference, the planform and the lift distribution of the optimized wing are plotted below.



An interesting result from the optimization is that the lift distribution of the wing is not elliptical, as would be predicted by aerodynamic theory. This is because aerodynamic theory does not consider the constraints imposed by structural limitations. A wing with a more ‘triangular’ lift distribution as shown above may be less optimal from the perspective of drag, but has lower tip deflection, and may be more optimal from a structures and weight standpoint. The optimization accurately captures these competing objectives and constraints.

**(b2.2)**

To evaluate the n-KKT conditions on the chosen wing design, we first evaluated which of the constraints were active. It was concluded that the tip deflection and fuel volume constraints were not active, although the fuel volume was only exceeded by 1/50 of the requirement. Therefore, the gradient had to be evaluated with respect to the two objectives (L/D, wing weight) and the other constraint (lift). The results are given below.

$x_i$	Normalized		Taper	Angles of attack					
	Span	Chord		a1	a2	a3	a4	a5	a6
$\frac{\partial LoD}{\partial x_i}$	18.37	-23.75	-14.93	-0.20	-1.09	-0.42	-0.35	-0.14	0.04
$\frac{\partial W_{wing}}{\partial x_i}$	37.12	22.70	15.02	0.00	0.00	0.00	0.00	0.00	0.00
$\frac{\partial L}{\partial x_i}$	351.08	258.32	119.46	7.53	14.85	10.50	4.80	1.77	0.27

To satisfy the n-KKT conditions, we would require:

$$\nabla LoD - \lambda_1 \nabla L = 0 \quad (1)$$

$$\nabla W_{wing} - \lambda_2 \nabla L = 0 \quad (2)$$

Where (1) is for the LoD objective, combined with the lift constraint, and (2) is for the Wwing objective, combined with the lift constraint. The least squared  $\lambda_1$  satisfying (1) is -0.0073, with a root mean squared of 33.4(solved using MATLABs lsqr function), and the least squared  $\lambda_2$  satisfying (2) is 0.1011, with a root mean squared of 4.1. Although for  $\lambda_2$  this is fairly close to zero (within order of magnitude)  $\lambda_1$  seems to be quite off, since it is not greater than zero, a KKT requirement. So it looks like LoD could still be optimized even further.